Electronic Supplementary Material (ESI) for Inorganic Chemistry Frontiers.

Supporting Information

EPR Spectroscopy Elucidates the Electronic Structure of [Fe^{V}(O)(TAML)] Complexes

Yujeong Kim,[†,‡] Jin Kim,[§] Linh K. Nguyen,[‡] Yong-Min Lee,[‡] Wonwoo Nam*[,‡] and Sun Hee Kim*[,†,‡]

[†] *Western Seoul Center, Korea Basic Science Institute (KBSI), Seoul 03759, Republic of Korea*

[‡] *Department of Chemistry and Nano Science, Ewha Womans University, Seoul 03760, Republic of Korea*

[§] *Department of Chemistry, Sunchon National University, Suncheon 57922, Republic of Korea*

*E-mail: wwnam@ewha.ac.kr, shkim7@kbsi.re.kr

Table of Contents

Experimental Section

Materials. All chemicals, obtained from Aldrich Chemical Co. and Tokyo Chemical Industry, were the best available purity and used without further purification unless otherwise indicated. Solvents were dried according to published procedures and distilled under argon prior to use.[S1] $H_2{}^{17}O$ (70% ^{17}O-enriched) was purchased from Cambridge Isotope Inc. (USA). Iodosylbenzene (PhIO) was prepared by a literature method.[S2] Na[Fe^{III}(TAML-1)] (H_4(TAML-1) = 3,4,8,9-tetrahydro-3,3,6,6,9-hexamethyl-1H-1,4,8,11-benzotetraazocyclotridecane-2,5,7,10-(6H,11H)-tetrone) was purchased from GreenOx Catalyst Inc. (Pittsburgh, PA, USA). Li[Fe^{III}(TAML-2)] (TAML-2 = $[(Me_2CNCOCMe_2NCO)_2CMe_2]^{4-}$ and H_4(TAML-2) = 2,2,5,5,6,6,9,9,12,12-decamethyl-1,4,7,10-tetraazacyclotridecane-3,8,11,13-tetraone) was prepared according to the literature method.[S3]

Generation and Characterization of 1 and 2. [Fe^{V}(O)(TAML-1)]$^{-}$ (**1**) was generated by adding idosylbenzene (PhIO; 20 equiv.) to Na[Fe^{III}(TAML-1)] in MeCN/TFE (v/v 9:1) at –40 °C.[S4] For the generation of [Fe^{V}(O)(TAML-2)]$^{-}$ (**2**), first, the starting iron(III) complex, Li[Fe^{III}(TAML-2)] was synthesized by reacting $Fe^{II}(OTf)_2$ with H_4(TAML-2) ligand in THF under an Ar atmosphere.[S3] Then, [Fe^{V}(O)(TAML-2)]$^{-}$ (**2**) was generated by adding PhIO (1.2 equiv.) to a solution of Li[Fe^{III}(TAML-2)] in MeCN/TFE (v/v 9:1) at -40 °C. ^{17}O-labeled **1** and **2** were produced by use of $PhI^{17}O$, which was generated by incubating $PhI^{16}O$ in the presence of ^{17}O-labeled water ($H_2{}^{17}O$, 5μL) in 50 μL for 20 min.

CW and Pulse EPR Spectroscopy. CW X-band (9.6 GHz) EPR spectra were collected on a Bruker EMX plus 6/1 spectrometer equipped with an Oxford Instrument ESR900 liquid He cryostat using an Oxford ITC 503 temperature controller. All spectra were collected with the following experimental parameters: microwave frequency, 9.64 GHz; microwave power, 0.03 mW; modulation amplitude, 10 G; time constant, 40.96 ms; 4 scans; temperature, 10 K.

X/Q-band pulse EPR data were obtained on a Bruker Elexsys E580 spectrometer and Cryogenic temperatures were achieved with an Oxford CF-935 cryostat and Oxford ITC temperature controller.

X-band pulse EPR data were acquired using a Bruker ER 4118X-MD5 dielectric ring resonator. The ^{17}O Davies ENDOR were performed using the π-*T*-π/2-τ-π-echo, with microwave pulse lengths of $t_{\pi/2}$ = 16 ns, t_{π} = 32 ns and an inter-pulse time of τ = 300 ns. In this sequence, the RF power is applied during the time *T* (20 μs) to drive nuclear spin transitions. The repetition time was 2 ms. The three-pulse ESEEM experiments were performed utilizing the three pulse sequence, π/2-τ-π/2-*T*-π/2-echo, with a pulse length of $t_{\pi/2}$ = 16 ns and inter-pulse times of τ = 250-270 ns and $T_{initial}$ = 70 ns. The HYSCORE experiments were carried out using a four pulse sequence, π/2-τ-π/2-t_1-π-t_2-π/2-τ-echo, with pulse length $t_{\pi/2}$ = 16 ns and t_{π} = 32 ns. The τ value was fixed but t_1 and t_2 were varied with a step size of 64 ns. A four step phase cycle was employed to eliminate unwanted echoes. The time domain spectra were baseline corrected, apodized with a Hamming window and zero-filled to 128 points before Fourier Transformation. The pulse measurements were conducted at 10 K.

Q-band pulse EPR data were collected using an EN5107D2 resonator. The Q-band ESE-EPR spectra were acquired using a pulse sequence, π/2-τ-π-echo, with a pulse length $t_{\pi/2}$ = 32 ns, t_{π} = 64 ns and τ = 200 ns. The Davies ENDOR were performed using the π-*T*-π/2-τ-π-echo, with microwave pulse lengths of $t_{\pi/2}$ = 32 ns, t_{π} = 64 ns and an inter-pulse time of τ = 200 ns. In this sequence, the RF power is applied during the time *T* (20 μs) to drive nuclear spin transitions. The repetition time was 5 ms. The Mims ENDOR were carried out using the pulse sequence, π/2-τ-π/2-*T*-π/2-echo, with microwave pulse lengths of 32 ns and an inter-pulse time of τ = 140 ns. In this sequence, RF power is applied during the time *T* (20 ms) to drive nuclear spin transitions. The repetition time was 5 ms. The pulse measurements were conducted at 8 K. All pulsed ENDOR spectra were obtained using stochastic sampling for better baseline of the spectra. The simulations of the EPR spectra were performed by EasySpin.[S5]

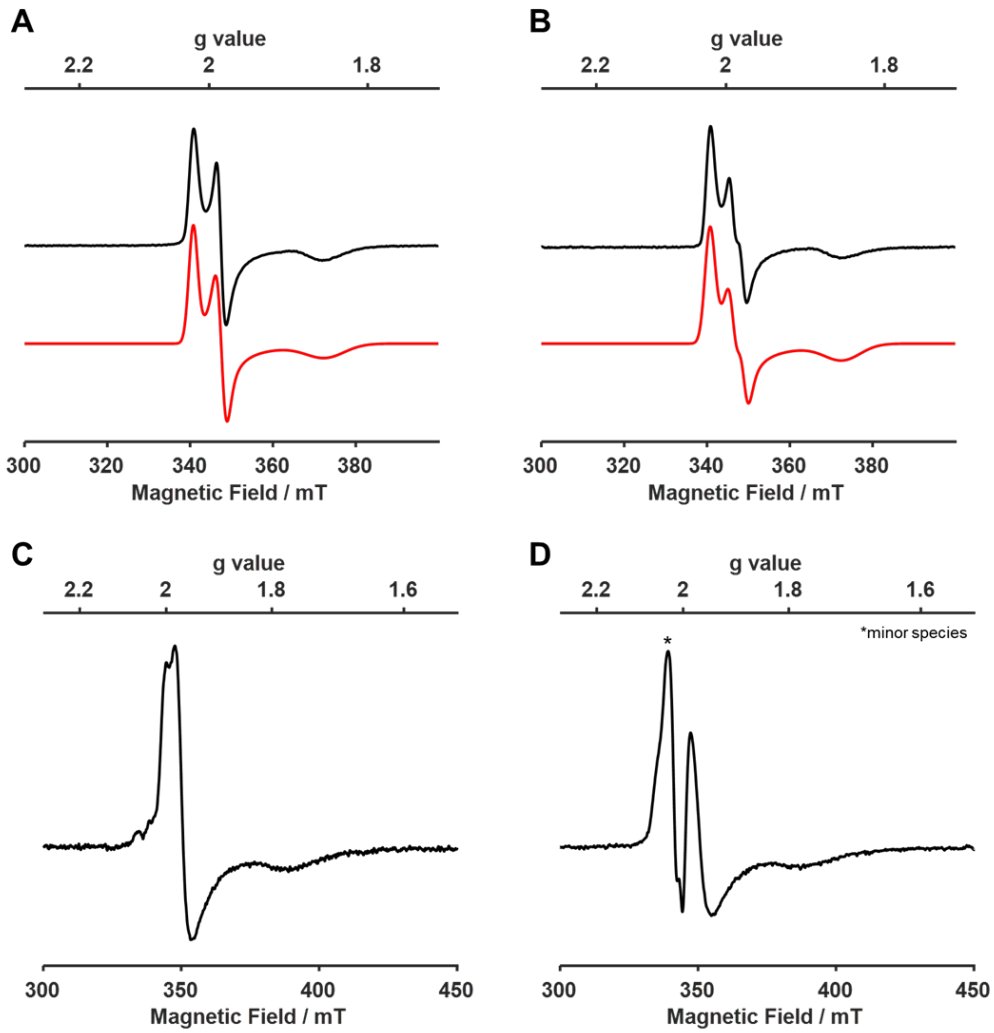

Figure S1. X-band CW-EPR spectra of (A) natural abundant ^{56}Fe-**2**, (B) ^{57}Fe-labeled **2**, (C) natural abundant ^{56}Fe-**1** and (D)^{57}Fe-labeled **1** (experimental: black, simulation: red). Experimental parameters: microwave frequency, 9.6 GHz; *T*, 20 K; modulation frequency, 100 KHz; modulation amplitude, 10 G. Simulation parameters: g = [2.022, 1.982, 1.845], A(^{57}Fe) = [-, 70, -] MHz for ^{57}Fe-labeled **2**. The peak marked with asterisk (*) indicates that a minor species is presented with g ~2.06.

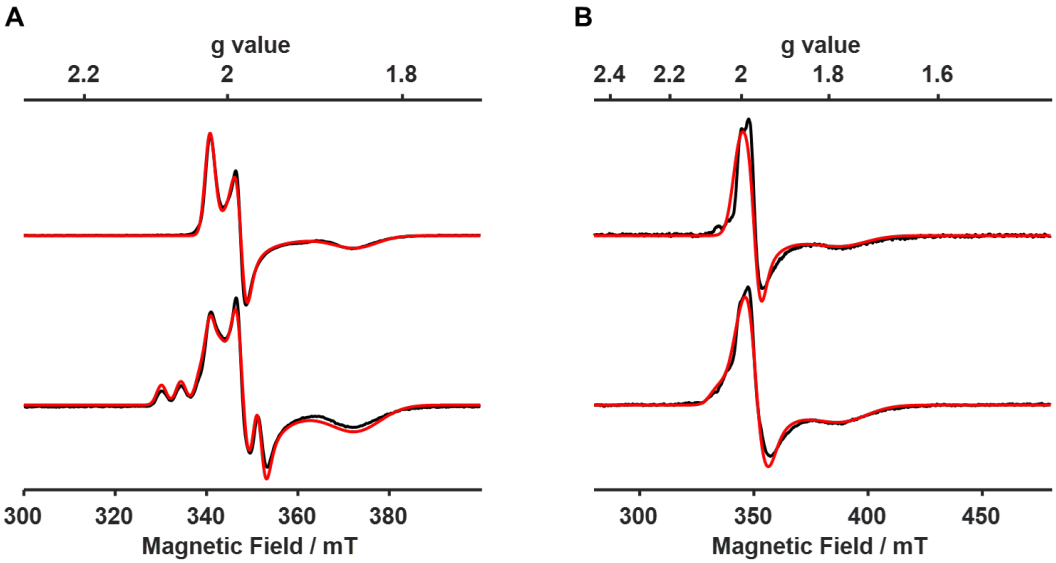

Figure S2. X-band CW EPR spectra of (A) natural abundant ^{16}O-**2** (upper) and ^{17}O-labeled **2** (lower), (B) natural abundant ^{16}O-**1** (upper) and ^{17}O-labeled **1** (lower) (experimental: black, simulation: red). Experimental parameters: microwave frequency, 9.6 GHz; *T*, 20 K; modulation frequency, 100 KHz; modulation amplitude, 10 G. The simulations were performed with the same spin Hamiltonian parameters as ^{17}O ENDOR simulations; (A) g = [2.022, 1.982, 1.845] and $A(^{17}\mathrm{O})$ = [–122, 22, 47] MHz for ^{17}O-labeled **2**; (B) g = [2.003, 1.965, 1.765] and $A(^{17}\mathrm{O})$ = [–119, 26, 57] MHz for ^{17}O-labeled **1**.

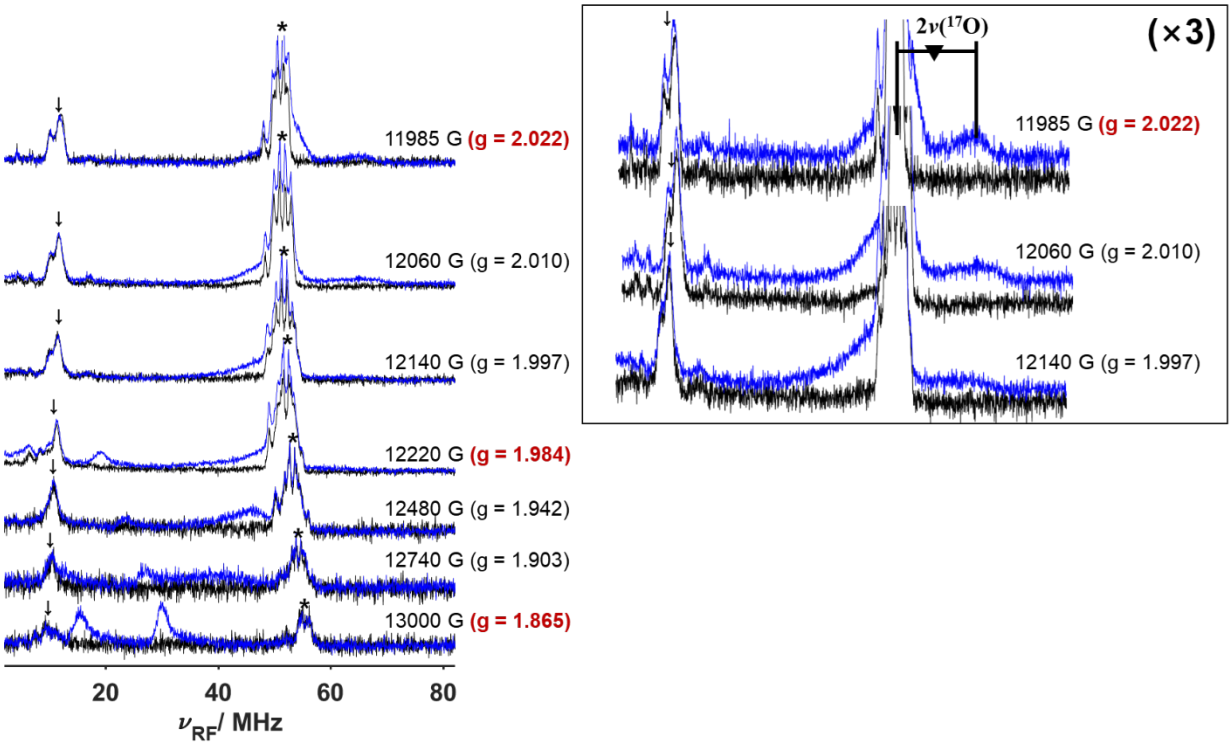

Figure S3. Q-band Davies ENDOR spectra of natural abundant ^{16}O-**2** (black) and ^{17}O-labeled **2** (blue). The inset shows the enlarged spectra of selective fields. The arrows (~15 MHz) indicate signals of ^{14}N(s) and the asterisks (~50 MHz) indicate signals of ^{1}H(s). Experimental conditions: microwave frequency, 33.9 GHz; *T*, 8 K; pulse sequence = 64-32-64 ns; τ = 200 ns; RF pulse = 20 μs.

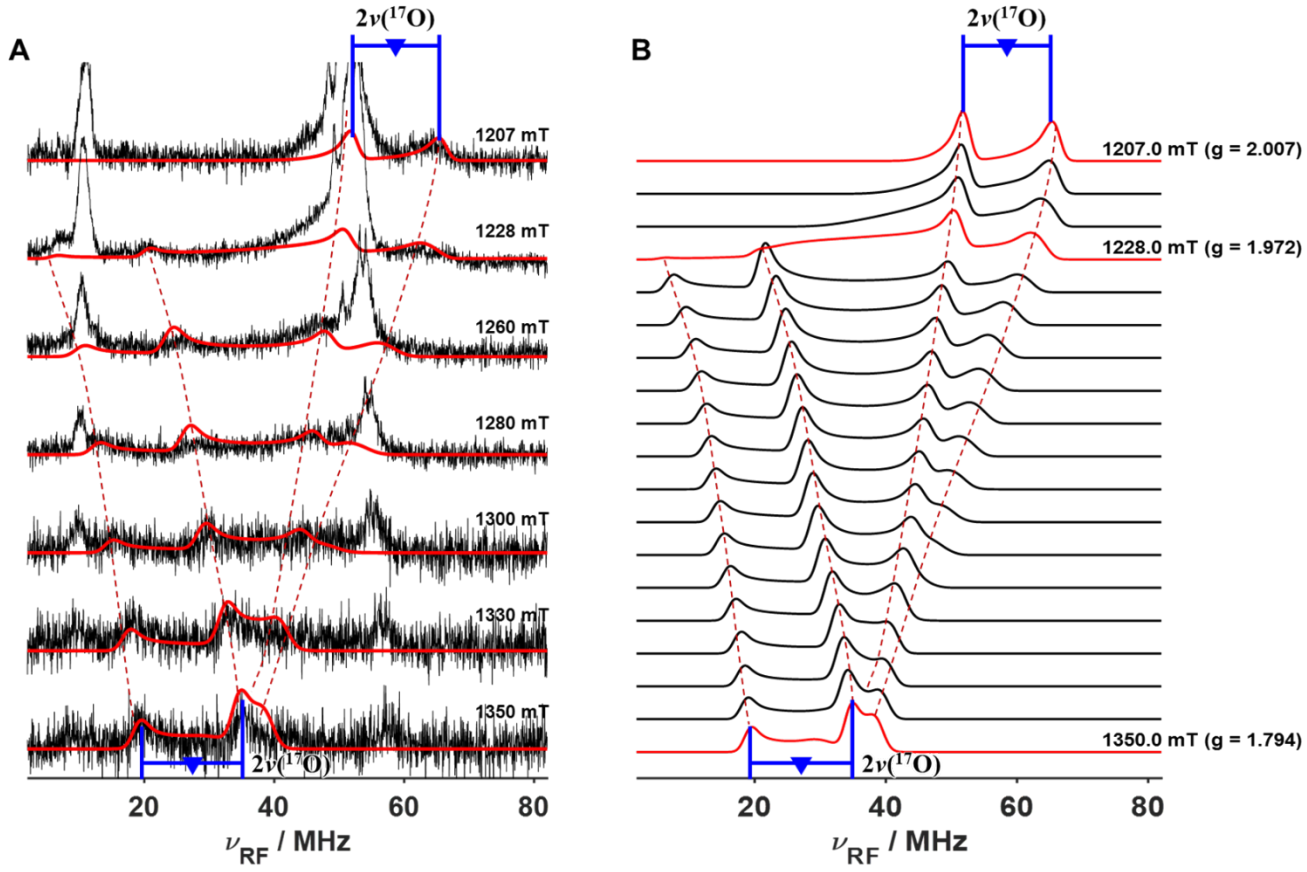

Figure S4. (A) Q-band Davies ENDOR spectra of ^{17}O-labeled **1** (experimental: black, simulation: red) and (B) the simulated field-dependent Davies ENDOR spectra. Experimental conditions: microwave frequency, 33.9 GHz; *T*, 8 K; pulse sequence = 64-32-64 ns; τ = 200 ns; RF pulse = 20 μs. Simulation parameters: g = [2.003, 1.965, 1.765] and $A(^{17}O)$ = [–119, 26, 57] MHz.

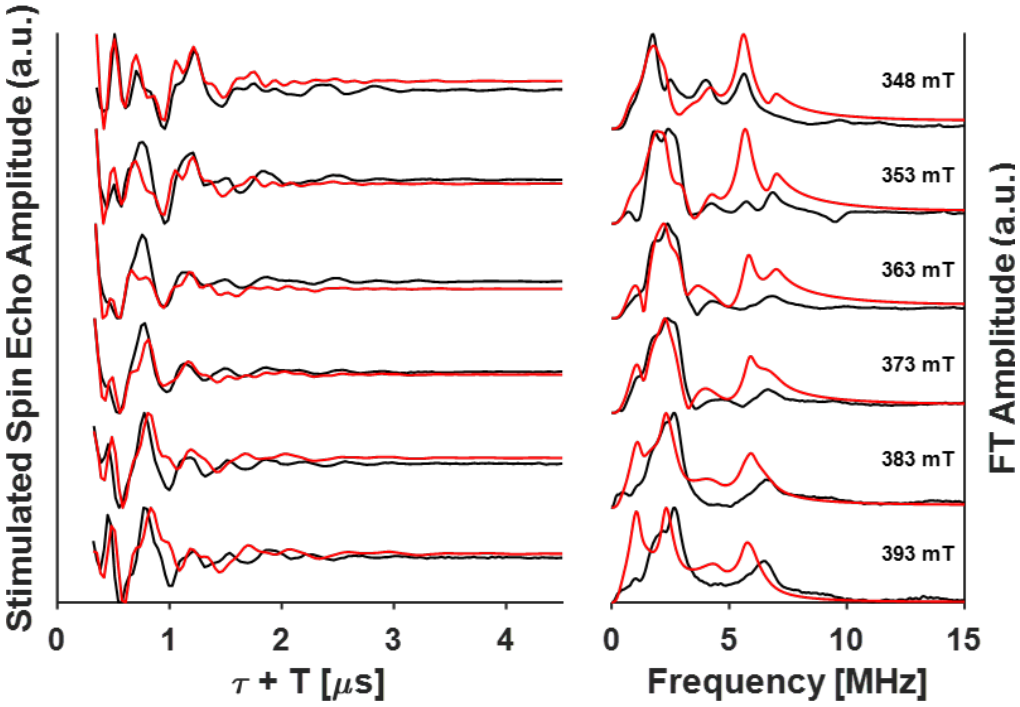

Figure S5. X-band ^{14}N three-pulse ESEEM spectra of **1 (**experimental: black, simulation: red). The time-domain spectra (left) and the frequency-domain (right) ESEEM spectra are shown. Experimental conditions: microwave frequency, 9.7 GHz; T, 10 K; pulse sequence = 16-16-16 ns; τ = 250-270 ns; $T_{initial}$ = 70 ns. Simulation parameters: g = [2.003, 1.965, 1.765]; A(^{14}N2) = [3.2, 3.2, 4.4] MHz; e^2Qq/h(^{14}N2) = 2.3 MHz; η = 0.7.

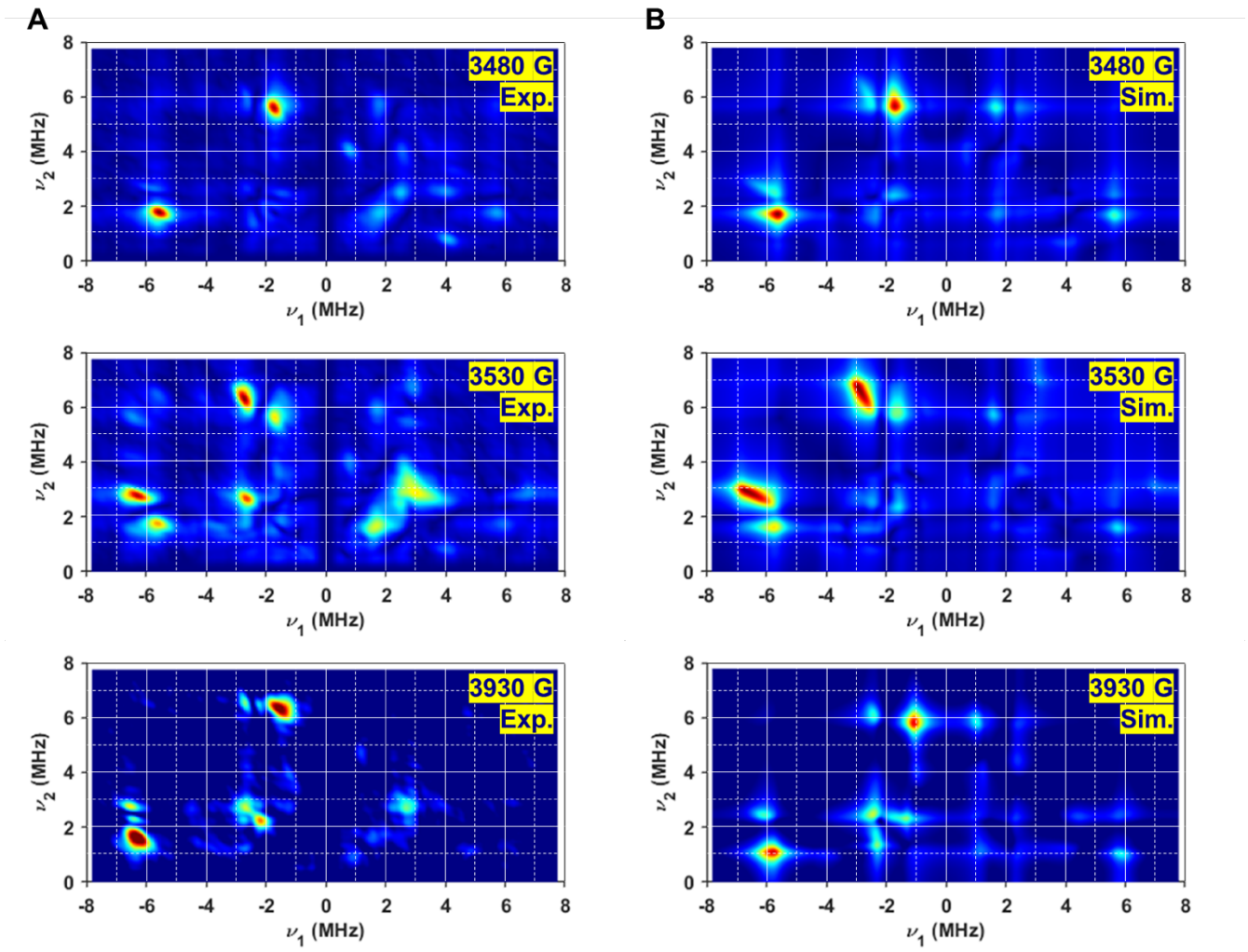

Figure S6. (A) X-band ^{14}N HYSCORE spectra of **1** and (B) their simulations. Experimental conditions: microwave frequency, 9.7 GHz; *T*, 10 K; pulse sequence = 16-16-32-16 ns; τ = 250-270 ns; *dx*, *dy* = 64 ns. Simulation parameters: g = [2.003, 1.965, 1.765]; $A(^{14}N2)$ = [3.2, 3.2, 4.4] MHz; $e^2Qq/h(^{14}N2)$ = 2.3 MHz; η = 0.7.

.

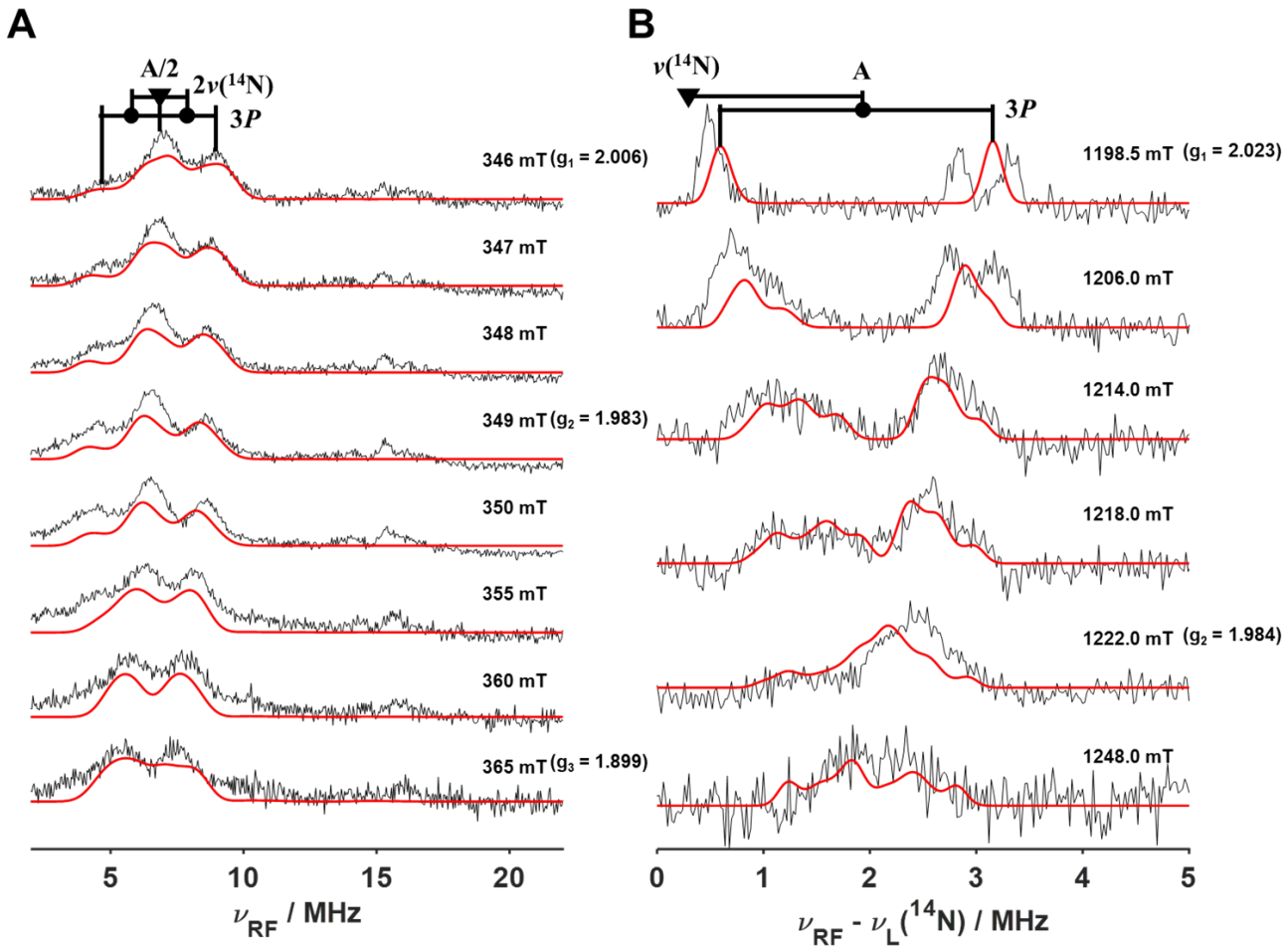

Figure S7. (A) X-band Davies ENDOR spectra of **2** and (B) Q-band Mims ENDOR spectra of **2** (experimental: black, simulation: red). Experimental conditions: (A) microwave frequency, 9.7 GHz; *T*, 10 K; pulse sequence = 32-16-32 ns; τ = 300 ns; RF pulse = 20 μs and (B) microwave frequency, 33.9 GHz; *T*, 8 K; pulse sequence = 32-32-32 ns; τ = 140 ns; RF pulse = 20 μs. Simulation parameters: (A) g = [2.022, 1.982, 1.845]; $A(^{14}\text{N1})$ = [12.0, 12.0, 160] MHz; $e^2Qq/h(^{14}\text{N1})$ = 2.2 MHz; η = 0.5 and (B) g = [2.022, 1.982, 1.845]; $A(^{14}\text{N2})$ = [3.6, 3.6, 4.2] MHz; $e^2Qq/h(^{14}\text{N2})$ = 2.2 MHz; η = 0.6.

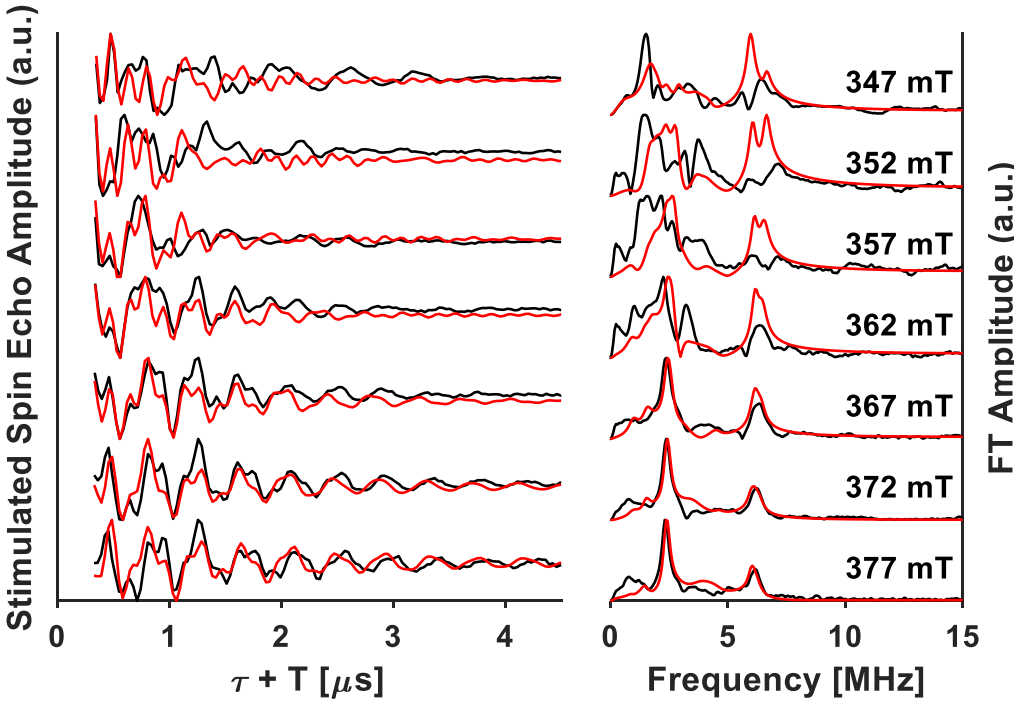

Figure S8. X-band ^{14}N three-pulse ESEEM spectra of **2**. The time-domain spectra (left) and the frequency-domain (right) ESEEM spectra are shown. Experimental conditions: microwave frequency, 9.7 GHz; T, 10 K; pulse sequence = 16-16-16 ns; τ = 250-270 ns; $T_{initial}$ = 70 ns. Simulation parameters: g = [2.022, 1.982, 1.845]; $A(^{14}N2)$ = [3.6, 3.6, 4.2] MHz; $e^2Qq/h(^{14}N2)$ = 2.2 MHz; η = 0.6.

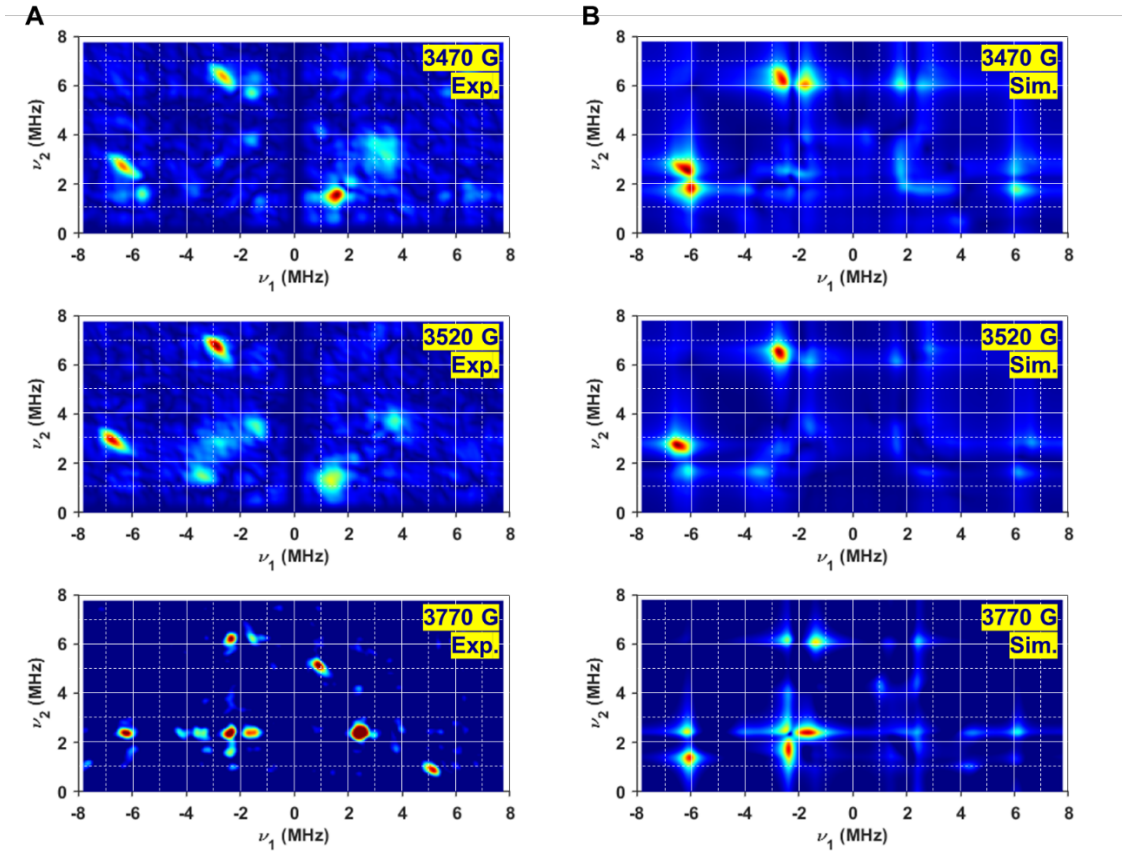

Figure S9. (A) X-band ^{14}N HYSCORE spectra of **2** and (B) their simulations. Experimental conditions: microwave frequency, 9.7 GHz; *T*, 10 K; pulse sequence = 16-16-32-16 ns; τ = 250-270 ns; *dx*, *dy* = 64 ns. Simulation parameters: *g* = [2.022, 1.982, 1.845]; *A*(^{14}N2) = [3.6, 3.6, 4.2] MHz; e^2Qq/h(^{14}N2) = 2.2 MHz; η = 0.6.

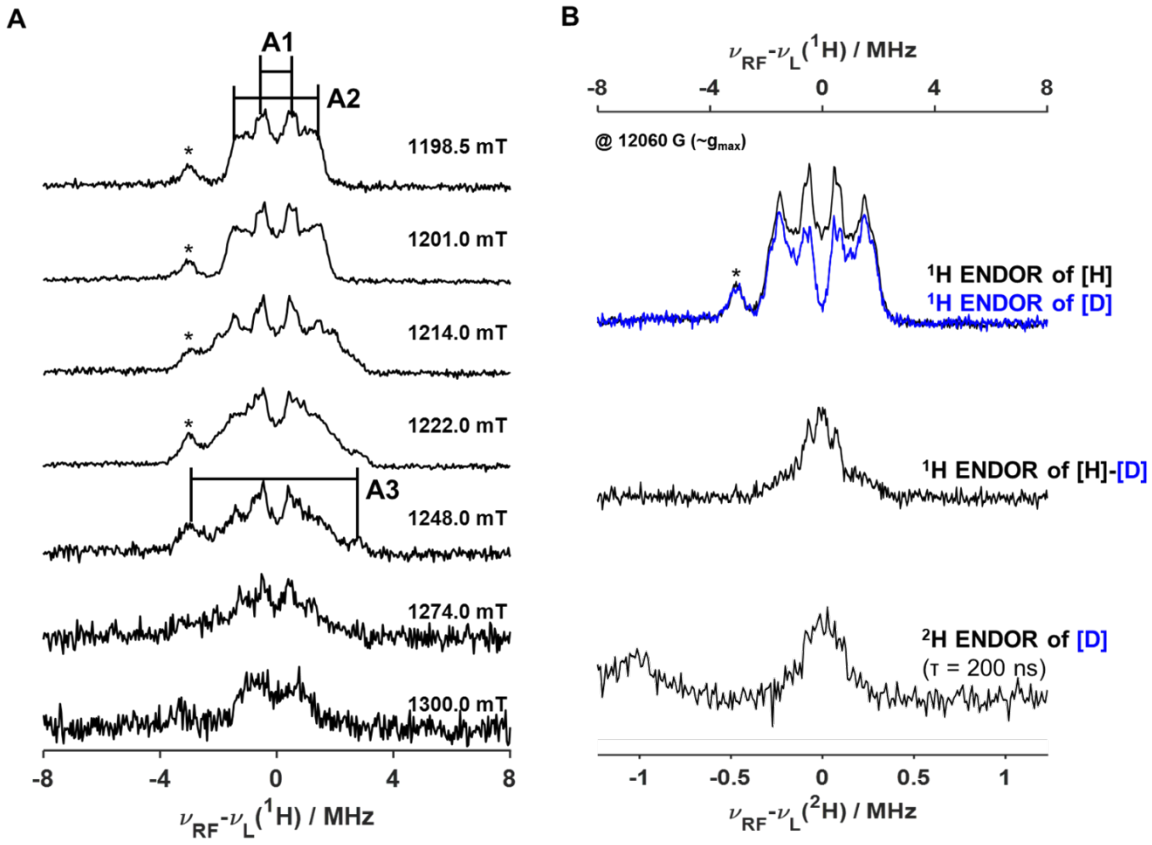

Figure S10. (A) Q-band ^{1}H Davies ENDOR spectra of **2** and (B) Q-band Davies ENDOR of **2** in [H]-solvent (upper, black line), in [D]-solvent (upper, blue line), subtracted spectrum in [H]-solvent – [D]-solvent (middle), and ^{2}H Mims ENDOR spectrum in [D]-solvent scaled by the ratio of nuclear *g*-values (lower). The asterisks indicate Larmor frequency of ^{19}F at each fields, which were originated from TFE solvent.

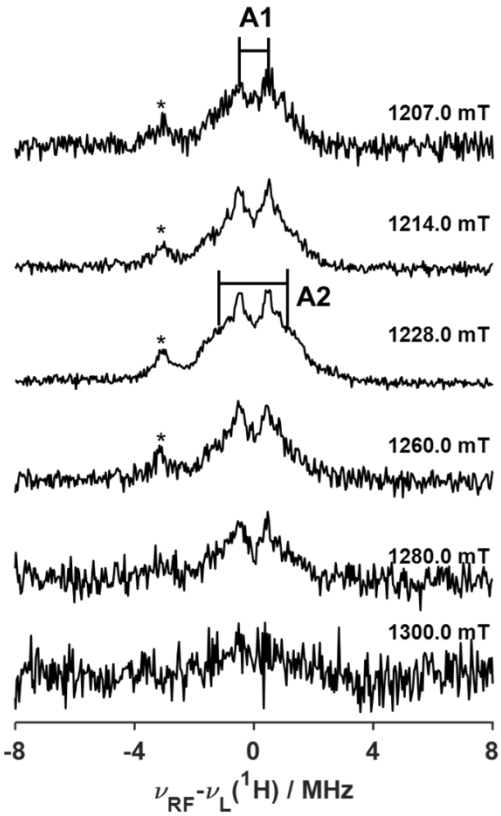

Figure S11. Q-band ^{1}H Davies ENDOR spectra of **1**. The asterisks indicate Larmor frequency of ^{19}F at each fields, which were originated from TFE solvent.

References

(S1) W. L. F. Armarego and C. L. L. Chai, *Purification of Laboratory Chemicals*. 6th ed., Pergamon Press, Oxford, UK, 2009.

(S2) (*a*) H. Saltzman and J. G. Sharefkin, *Organic Syntheses*; Wiley: New York, 1973, Vol. *V*; p 658; (*b*) P. Dauban, L. Saniere, A. Tarrade, and R. H. Dodd, Copper-Catalyzed Nitrogen Transfer Mediated by Iodosylbenzene PhI=O, *J. Am. Chem. Soc.*, 2001, **123**, 7707−7708.

(S3) M. A. DeNardo, M. R. Mills, A. D. Ryabov and T. J. Collins, Unifying Evaluation of the Technical Performances of IronTetraamido Macrocyclic Ligand Oxidation Catalysts, *J. Am. Chem. Soc.*, 2016, **138**, 2933−2936.

(S4) F. T. de Oliveira, A. Chanda, D. Banerjee, X. Shan, S. Mondal, L. Que, Jr., E. L. Bominaar, E. Münck, T. J. Collins, Chemical and Spectroscopic Evidence for an Fe^{V}-Oxo Complex, *Science*, 2007, **315**, 835−838.

(S5) S. Stoll and A. Schweiger, EasySpin, a Comprehensive Software Package for Spectral Simulation and Analysis in EPR, *J. Magn. Reson.*, 2006, **178**, 42–55.